



HAL
open science

High-frequency rotational losses in different Soft Magnetic Composites (SMC)

Olivier de La Barrière, Carlo Appino, Carlo Ragusa, Fausto Fiorillo, F. Mazaleyrat,
M. Lobue

► **To cite this version:**

Olivier de La Barrière, Carlo Appino, Carlo Ragusa, Fausto Fiorillo, F. Mazaleyrat, et al.. High-frequency rotational losses in different Soft Magnetic Composites (SMC). *Journal of Applied Physics*, 2014, 115 (17), pp.17A331-1-17A331-3. <10.1063/1.4865974>. <hal-01100338>

HAL Id: hal-01100338

<https://hal.science/hal-01100338v1>

Submitted on 6 Jan 2015

HAL is a multi-disciplinary open access archive for the deposit and dissemination of scientific research documents, whether they are published or not. The documents may come from teaching and research institutions in France or abroad, or from public or private research centers.

L'archive ouverte pluridisciplinaire HAL, est destinée au dépôt et à la diffusion de documents scientifiques de niveau recherche, publiés ou non, émanant des établissements d'enseignement et de recherche français ou étrangers, des laboratoires publics ou privés.



HAL Authorization

High-frequency rotational losses in different Soft Magnetic Composites (SMC)

O. de la Barrière^{1a}, C. Appino², C. Ragusa³, F. Fiorillo², F. Mazaleyrat¹ and M. LoBue¹

¹SATIE, ENS Cachan, CNRS, UniverSud, 61 av du President Wilson, F-94230 Cachan, France

²Istituto Nazionale di Ricerca Metrologica (INRIM), Torino, Italy

³Dipartimento di Ingegneria Elettrica, Politecnico di Torino, C.so Duca degli Abruzzi 24, 10129 Torino, Italy

^a Corresponding author: barriere@satie.ens-cachan.fr

1 **Abstract**

2 The isotropic properties of Soft Magnetic Composites (SMC) favor the design of new machine
3 topologies and their granular structure can induce a potential decrease of the dynamic loss component
4 at high frequencies. This paper is devoted to the characterization of the broadband magnetic losses of
5 different SMC types under alternating and circular induction. The investigated materials differ by their
6 grain size, heat treatment, compaction rate and binder type. It is shown that, up to peak polarization $J_p =$
7 1.25 T, the ratios between the rotational and the alternating loss components (classical, hysteresis, and
8 excess) are quite independent of the material structural details, quite analogous to the known behavior
9 of nonoriented steel laminations. At higher inductions, however, this is no more the case. It is observed,
10 in particular, that the J_p value at which the rotational hysteresis loss attains its maximum, related to the
11 progressive disappearance of the domain walls under increasing rotational fields, decreases with the
12 material susceptibility.

13

14 I. INTRODUCTION

15 Embedded applications, such as hybrid vehicles or aircraft systems, are a challenge for machine
16 designers. Indeed, the mass of these systems, and then the actuator torque density, are crucial
17 parameters. Possible solution call either for the increase of the actuator working frequency, in order to
18 improve the torque density [1], or the design of non-conventional machine topologies such as claw pole
19 machines [2]. For both alternatives, the technological limitations of conventional laminated magnetic
20 materials may be reached. Actually, the classical eddy current losses can become too important at high
21 frequencies, while laminated materials only allow flux circulation in the lamination plane, and
22 therefore are not suitable for claw pole machines with 3D flux paths [2]. Soft Magnetic Composites can
23 be a satisfying solution, because their granular structure brings about a significant reduction of the
24 classical losses [3], while exhibiting good isotropic properties [4]. Consequently, there is a clear
25 necessity to provide machine designers loss results and models for such materials under multi-
26 dimensional induction excitations.

27 The relatively low susceptibility of SMC, and the necessity to reach the range of frequencies for
28 which these materials are designed, can make the experiments particularly difficult. For laminations,
29 most of the 2D induction loss results are provided for the industrial frequency of 50 Hz [5], or up to
30 200 Hz [6]. On the contrary, SMC require testing in the kilohertz range [4]. A few papers present such
31 results. In [4], the peak induction of 0.54 T has been reached for a maximum frequency of 1000 Hz
32 under 3D induction loci, using a special winding of the measurement setup (the number of turns is
33 decreased while the frequency increases). In [7] loss results under alternating and circular inductions in
34 a SMC disk sample up to 1.25 T at 1000 Hz are proposed, using a specially designed three phase
35 magnetizer. However, contrary to the alternating induction case [8], no comparative study of the loss
36 under multi-dimensional induction waveforms in different SMC samples (with different grain sizes,
37 different preparation methods or binder...) has been performed so far. This makes difficult the choice

38 of the best SMC for a given application.

39 In this paper, three different SMC samples have been experimentally characterized under alternating
40 and circular induction loci up to the kilohertz range, using the system presented in [7]. In the following
41 we discuss first experiments made up to peak polarization $J_p = 1.25$ T. It is shown that, in spite of
42 different loss values and behaviors in the different materials, the ratio of the circular to the alternating
43 hysteresis loss components appears to be quite independent of the sample, the same being also true for
44 the excess loss. We consider then the material behavior at higher peak polarizations, experimentally
45 showing that the J_p value at which the hysteresis loss under circular polarization reaches its maximum
46 is correlated with the material susceptibility.

47 **II. EXPERIMENTAL**

48 **A. Measurement setup**

49 The measurement setup for SMC testing under 2D induction is similar to the one used in [7]. Disk-
50 shaped samples have been pressed directly to the final size (diameter 80 mm, thickness 3 mm), i.e. no
51 cutting has been made. For mechanical reasons, samples thinner than 3 mm could not be manufactured.
52 The disk samples have been centered in the bore of a three phases/two poles magnetizer endowed, for
53 maximum field homogeneity, with three slots per pole and per phase and a toroidal winding,
54 minimizing the copper losses and avoiding overhangs crossing. The geometry of the magnetizer has
55 been optimized by 3D finite elements, in order to reach the best induction-frequency combination
56 under power supply by a CROWN AUDIO 5000VZ linear amplifier.

57 The loss measurements were performed out by the fieldmetric method (double B-coil and H-coil
58 [7]). The measurement zone is a square of 20 mm at the center of the sample, offering a good
59 compromise between signal strength and induction homogeneity, the latter being verified by a finite
60 element computation, as made in [9]). The H-coils have been tested by an impedance analyzer to check
61 that the capacitive effects between turns were negligible in the measurement range of frequencies.

62 Induction loci are controlled thanks to a feedback algorithm [10]. For the case of alternating sinusoidal
63 induction, the loss measurements have been carried out along two perpendicular directions and the
64 results have been averaged. For measurements under circular polarization, averaging is made of the
65 loss figures obtained for clockwise and counterclockwise rotation.

66 B. Investigated SMC materials

67 In this paper, three kinds of commercial SMC are characterized and compared. These materials are
68 made of pure iron grains with electrical conductivity $\sigma_{\text{Fe}}=9.93 \cdot 10^6$ S/m (detailed information is given in
69 Table I). The first two materials have been obtained using inorganic binders and are heat-treated at
70 much higher temperature than Material 3, where an organic binder is used. The compacting pressure is
71 also higher for the first two materials. The micrographic inspection shows that Material 1 has much
72 larger average grain size than Materials 2 and 3 (167 μm versus 46 μm and 57 μm , respectively).
73 Material 3 shows quite larger dispersion of the grain size than Materials 1 and 2. The higher magnetic
74 susceptibility of Material 1 makes it suitable for applications in electrical machines. Materials 2 and 3,
75 with smaller grain size and higher resistivity (because of their lower density, the grain-to-grain contacts
76 are reduced), have lower classical eddy current losses. They are consequently more suitable for high-
77 frequency applications, such as power electronics inductors or very high speed machines [11].

78 III. ROTATIONAL AND ALTERNATING LOSSES UP TO $J_p = 1.25$ T

79 In this Section, energy losses measured under circular and alternating sinusoidal induction are
80 provided up to a few kHz for low and medium induction levels and maximum peak polarization $J_p =$
81 1.25 T. Using a classical loss model, it is possible to separate the loss components and analyze for each
82 material the ratios between hysteresis loss under circular and alternating conditions
83 $R_{\text{hyst}}(J_p) = W_{\text{hyst}}^{(\text{CIRC})}(J_p) / W_{\text{hyst}}^{(\text{ALT})}(J_p)$, and the excess loss ratios $R_{\text{exc}}(J_p) = W_{\text{exc}}^{(\text{CIRC})}(J_p, f) / W_{\text{exc}}^{(\text{ALT})}(J_p, f)$.

84 A. Measurements

85 For each material, loss measurements at the polarization levels $J_p = 0.2$ T, 0.5 T, 1 T, and 1.25 T
86 have been carried out under circular and alternating sinusoidal induction loci. The results are shown in
87 Fig. 1 for $J_p = 0.5$ T, 1 T, and 1.25 T. Material 1 has the highest dynamic loss (both under circular and
88 alternating polarization). This is chiefly due to its large grain size, which is responsible for a significant
89 mesoscopic classical loss [8]. The small grain-sized Materials 2 and 3, present in fact quite reduced
90 dynamic loss. This has, however, a counterpart in a higher hysteresis (quasi-static) loss. It is remarked
91 that these behaviors, typically observed under alternating field, equally hold for circular polarization. In
92 the following Section we will more precisely show that the ratios of rotational to alternating loss
93 components (hysteresis, excess, and classical loss) are to a good extent independent of the material.

94 The effect of the heat treatment is apparent on comparing Materials 2 and 3. Although Material 2
95 has smaller grain size and is manufactured with a higher compaction pressure (Table 1), it has lower
96 hysteresis loss under identical excitation conditions. Material 2 is prepared with inorganic binder and is
97 heat-treated beyond 500°C, while Material 3, with its organic binder, is cured at low temperatures
98 (200°C), to avoid binder deterioration. Higher hysteresis loss are inevitably associated with Material 3,
99 because, as explained in [12], the heat treatment helps relieving the residual stresses arising during the
100 compaction process.

101 B. Loss separation under alternating and circular polarization

102 The starting point of the loss separation is the classical loss computation. The main assumption is,
103 like in [8], that the classical loss remains confined at the scale of the single grain (we speak of
104 microscopic classical loss), and that eddy currents circulating on a larger scale because of random
105 grain-to-grain contacts are negligible. This is a reasonable assumption when considering, as in the
106 present case a few millimeter thick samples [8]. The classical loss computation under alternating field
107 conditions $W_{\text{class}}^{(\text{ALT})}(J_p, f)$ is carried out using the microscopic eddy current loss computation proposed

108 in [13], taking into account the grain size and shape dispersion observed on micrographs. Following
109 [6], the classical loss under circular field conditions is obtained doubling the classical alternating loss,
110 so that the ratio $R_{\text{class}} = W_{\text{class}}^{(\text{CIRC})}(J_p, f) / W_{\text{class}}^{(\text{ALT})}(J_p, f) = 2$.

111 The ratios of the circular to the alternating hysteresis loss $R_{\text{hyst}}(J_p)$ (this loss component being
112 obtained by extrapolating the total loss to zero frequency [7]) are given versus J_p in Fig. 2 for each
113 material. $R_{\text{hyst}}(J_p)$ decreases with J_p [7], with the quite interesting property of being little dependent on
114 the material type. This quite in agreement with previous results obtained in Fe-Si laminations having
115 different grain size [14].

116 A similar comparison for the excess loss ratio $R_{\text{exc}}(J_p)$ has been carried out (Fig. 3). It has been
117 experimentally shown in [7] that this ratio is almost frequency independent. A somewhat similar
118 conclusion can be drawn for Materials 1 and 3 (Fig. 3), although the results obtained in Material 3 are
119 very noisy because of the small amount of dynamic loss. Material 2 has so small dynamic loss that an
120 accurate evaluation of the dynamic loss component is not possible.

121 **IV. HYSTERESIS LOSSES UP TO 1.6 T**

122 In this section, higher peak polarization values, up to $J_p=1.6$ T, are considered, both under circular
123 and alternating flux, for the three materials. The actual measuring frequency $f = 50$ Hz can be
124 considered as quasi-static in these materials, given the correspondingly negligible dynamic loss
125 contribution. Thus, we can assume $W_{\text{tot}}(J_p, 50 \text{ Hz}) = W_{\text{hyst}}(J_p)$.

126 Quite remarkably, it is observed that the rotational hysteresis loss $W_{\text{hyst}}^{(\text{CIRC})}(J_p)$ attains its maximum
127 at different J_p values in the different materials. In particular, $J_{p,\text{MAX}}$ drifts from 1.5 T to 1.25 T on going
128 from Material 1 to Material 3. A similar trend cannot be observed in the conventional nonoriented Fe-
129 Si laminations, where $W_{\text{hyst}}^{(\text{CIRC})}(J_p)$ invariably attains a maximum value close to $J_p = 1.5$ T [14]. The
130 fact that $W_{\text{hyst}}^{(\text{CIRC})}$ passes through a maximum value, to eventually drop to zero value on the approach
131 to saturation, points to the contribution of the coherent magnetization rotations, which are reversible in

132 nature, becoming significant with respect to the domain wall processes. It is apparent that the evolution
133 of $W_{\text{hyst}}^{(\text{CIRC})}(J_p)$ shown in Fig. 4 is a peculiar consequence of the granular structure of the SMC
134 materials and the role of the internal demagnetizing fields. We actually see in Table I that the drift of
135 the maximum of $W_{\text{hyst}}^{(\text{CIRC})}(J_p)$ correlates with a similar drift of the material susceptibility, in turn
136 strictly depending on the material density. It is clear, looking also at the shape of the hysteresis loops,
137 that the susceptibility is chiefly determined by the internal demagnetizing fields, which are pretty
138 strong, in view of the non-negligible thickness of the non-magnetic grain boundary layer. Lower
139 susceptibility SMC are associated with thicker layers, higher average internal demagnetizing effects,
140 and broader distribution of the local demagnetizing coefficients. Very broad distribution of the internal
141 demagnetizing fields implies that higher applied fields are required for achieving any given J_p . It
142 happens then that the domain wall processes are quite not exhausted, contrary to magnetic laminations,
143 when the applied field is high enough to engender coherent rotations in the softer (i.e. surrounded by
144 thinner layers) grains. The coherent rotations tend eventually to occur at lower inductions in the lower
145 susceptibility SMC materials, bringing with them a similar trend for the turning point of $W_{\text{hyst}}^{(\text{CIRC})}(J_p)$.

146 V. CONCLUSION AND PERSPECTIVES

147 In this paper, measurements under alternating and circular inductions in different SMC types (grain
148 size, binder, preparation) have been proposed, up to 3 kHz. The loss components have been separated,
149 and it has been shown that the ratios of these components, measured under circular and alternating
150 polarization, do not significantly depend on the material type.

151 The alternating and rotational hysteresis losses have also been measured up to high inductions ($J_p =$
152 1.6 T). It has been shown that the rotational hysteresis loss $W_{\text{hyst}}^{(\text{CIRC})}(J_p)$ passes through its maximum
153 value at lower J_p values in lower susceptibility materials. This effect, never observed in the
154 conventional soft magnetic laminations, can be qualitatively justified by taking into account that the
155 susceptibility in SMC is chiefly determined by the thickness of the non-magnetic grain boundaries, that

156 is, the strength of the internal demagnetizing fields. The higher these fields, as occurring in lower
157 density materials, the broader their distribution and the stronger the field to be applied to reach a given
158 J_p value. This inevitably leads to earlier appearance of coherent magnetization rotations with respect to
159 denser materials and anticipated fall of $W_{\text{hyst}}^{(\text{CIRC})}(J_p)$ versus J_p .

160

- 162 [1] D.G. Dorrell, M. Hsieh, and A.M. Knight, *IEEE Trans. Magn.* 48(2), 835-838 (2012).
163 [2] Y. Guo, J.G. Zhu, Z.W. Lin, H. Lu, X. Wang, J. Chen, *J. Appl. Phys.* 103(7), 07F118 (2008).
164 [3] C. Appino, O. de la Barriere, F. Fiorillo, M. LoBue, F. Mazaleyrat, C. Ragusa, *J. Appl. Phys.*
165 113(7), 17A322 (2013).
166 [4] Y. Li, J. Zhu, Q. Yang, Z.W. Lin, Y. Guo, Y. Wang, *IEEE Trans. Magn.* 46(6), 1971-1974 (2010).
167 [5] M. Enokizono, T. Suzuki, J. Sievert, and J. Xu, *IEEE Trans. Magn.* 26(5), 2562-2564 (1990).
168 [6] C. Appino, F. Fiorillo, and C. Ragusa, *J. Appl. Phys.* 105(7), 07E718 (2009).
169 [7] O. de la Barriere, C. Appino, F. Fiorillo, C. Ragusa, M. Lecrivain, L. Rocchino, H. Ben Ahmed,
170 M. Gabsi, F. Mazaleyrat, M. LoBue, *J. Appl. Phys.* 111(7), 07E325 (2012).
171 [8] O. de la Barriere, C. Appino, F. Fiorillo, C. Ragusa, H. Ben Ahmed, M. Gabsi, F. Mazaleyrat, M.
172 LoBue, *J. Appl. Phys.* 109(7), 07A317 (2011).
173 [9] N. Nencib, A. Kedous-Lebouc, and B. Cornut, *IEEE Trans. Magn.* 31(6), 3388-3390 (1995).
174 [10] C. Ragusa and F. Fiorillo, *J. Magn. Magn. Mat.* 304(2), e568-e570 (2006).
175 [11] A. Chebak, P. Viarouge, and J. Cros, *IEEE Trans. Magn.* 45(3), 952-955 (2009).
176 [12] H. Shokrollahi and K. Janghorban, *Journal of materials processing technology* 187(1), 1-12
177 (2007).
178 [13] O. de la Barriere, C. Appino, F. Fiorillo, C. Ragusa, M. Lecrivain, L. Rocchino, H. Ben Ahmed,
179 M. Gabsi, F. Mazaleyrat, M. LoBue, *IEEE Trans. Magn.* 49(4), 1318-1326 (2013).
180 [14] C. Ragusa, C. Appino, and F. Fiorillo, "Comprehensive investigation of alternating and rotational
181 losses in non-oriented steel sheets," *Przeegląd Elektrotechniczny*, vol. 85, pp. 7-10, 2009.
182

183

Table captions

184 Table 1: Main physical properties of the SMC materials used in this work.

185

Figures captions

186 Fig. 1: Total energy loss per cycle under circular and alternating sinusoidal induction loci as a
187 function of the frequency f , for the induction peak values $J_p=0.5$ T, 1 T, and 1.25 T.

188 Fig. 2: Hysteresis loss ratio $R_{\text{hyst}}(J_p)=W_{\text{hyst}}^{(\text{circ})}(J_p)/W_{\text{hyst}}^{(\text{alt})}(J_p)$ versus the peak polarization J_p , for
189 each material.

190 Fig. 3: Excess loss ratio $R_{\text{exc}}(J_p)=W_{\text{exc}}^{(\text{circ})}(J_p, f)/W_{\text{exc}}^{(\text{alt})}(J_p, f)$ versus the peak polarization J_p , for each
191 material, at three different frequencies ($f=100$ Hz, 500 Hz, and 1000 Hz).

192 Fig. 4: Measured loss $W_{\text{tot}}(J_p, f=50\text{Hz})$ under circular and alternating sinusoidal induction loci, in
193 function of the peak value J_p .

194

Tables

Material	Density (kg/m ³)	Compacting pressure (MPa)	Binder	Heat treatment		Mean grain size (μm)	Electrical resistivity (μΩm)	χ_r^b
				Temp. (°C)	Time (minutes)			
1	7450	800	Inorganic	530	30	167 (rsd ^c =1.1%)	700	440
2	7260	800	Inorganic	530	30	46 (rsd=1.2%)	7000	200
3	7110	600	Organic	200	30	57 (rsd=1.8%)	900	140

Table 1

^b Measured relative magnetic susceptibility, defined for an alternating field as $\chi_r = J_p / (\mu_0 H_p)$, J_p is the peak polarization chosen equal to 1 T, H_p is the corresponding peak magnetic field under static conditions.

^c The abbreviation rsd means “relative standard deviation“, which is, in statistics, the ratio between the standard deviation and the mean of a set of data.

Figures

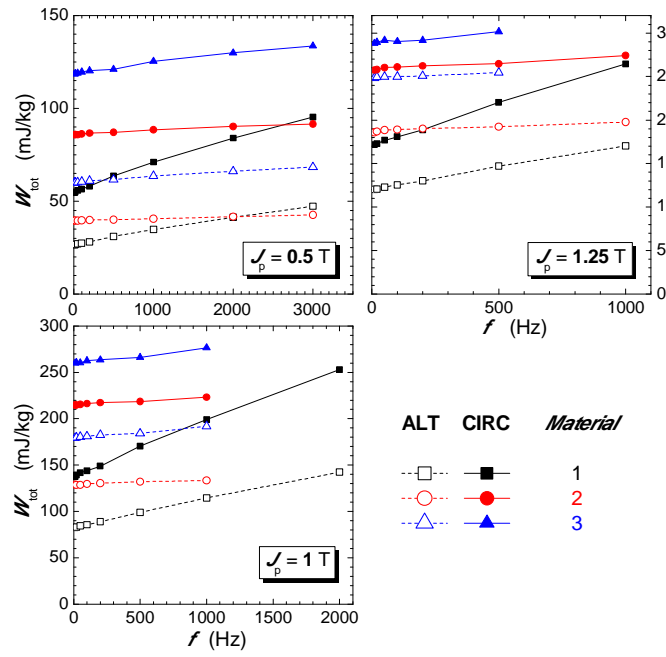


Fig. 1

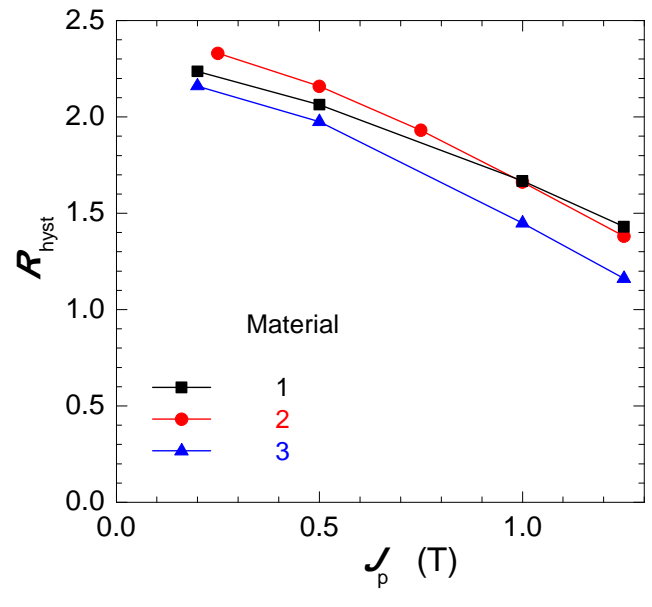


Fig. 2

200
201

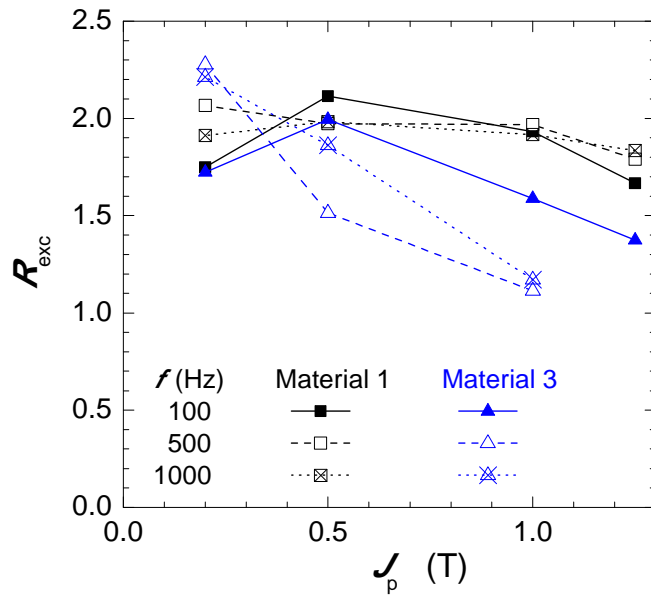


Fig. 3

202

203

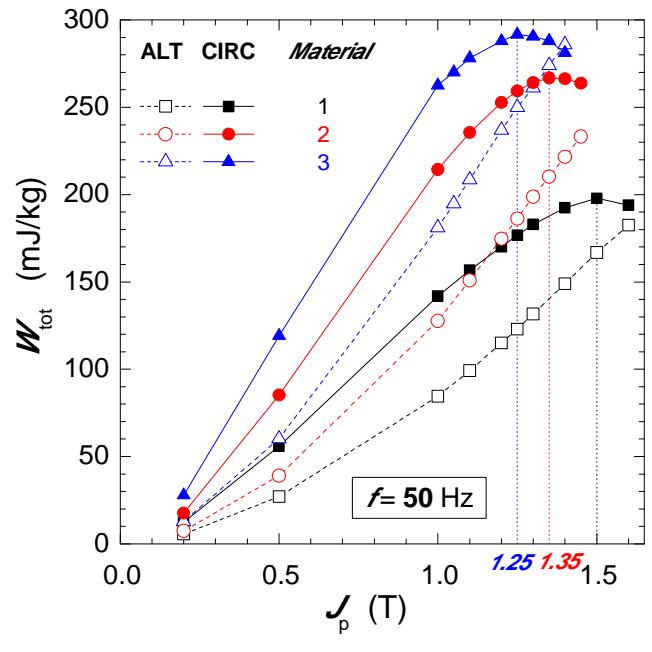


Fig. 4

204
205